Volume 57(8): 721–730, 2009
Journal of Histochemistry & Cytochemistry
http://www.jhc.org

The Journal of Histochemistry & Cytochemistry

ARTICLE

Apoptosis and Desquamation of Urothelial Cells in Tissue Remodeling During Rat Postnatal Development

Andreja Erman, Daša Zupančič, and Kristijan Jezernik

Institute of Cell Biology, Faculty of Medicine, Ljubljana, Slovenia

SUMMARY Postnatal rat urothelium was studied from day 0 to day 14, when intense cell loss as part of tissue remodeling was expected. The morphological and biochemical characteristics of urothelial cells in the tissue and released cells were investigated by light and electron microscopy, by terminal deoxynucleotidyl transferase–mediated dUTP nick end labeling (TUNEL) assay, by annexin V/propidium iodide assay, and by immunofluorescent detection of active caspases and tight-junction protein occludin. Intense apoptosis and massive desquamation were detected between postnatal days 7 and 10. During this period, active caspases and TUNEL-positive cells were found in the urothelium. Disassembled cell–cell junctions were detected between cells. The majority of desquamated cells expressed no apoptotic cell morphology, but were active caspase positive and TUNEL positive. Ann+/PI− apoptotic bodies and desquamated Ann+/PI+ cells were detected in the lumen. These results indicate that apoptosis and desquamation participate in urothelial cell loss in the rat early postnatal period, indispensable for fast urothelial remodeling during development.

(J Histochem Cytochem 57:721–730, 2009)

KEY WORDS
rat urothelium
postnatal development
desquamation
apoptosis

THE LUMINAL SURFACE of rat urinary bladder is covered by a highly specialized, three-layered urothelium, made up of basal, intermediate, and superficial cell layers. Superficial cells, which are in contact with toxic and hypertonic urine, have a specialized apical plasma membrane and well-developed tight junctions. The urothelium is a stable tissue resistant to mechanical forces; it has already been demonstrated, however, that it responds with increased desquamation to various stress factors, such as prolonged illumination, stress hormones, heat, or endotoxin instillation. Many studies of the urothelium have focused on desquamation as a consequence of pathological conditions (Aronson et al. 1988; Dalal et al. 1994; Veranič and Jezernik 2000, 2001). Much less is known about desquamation of urothelial cells under physiological conditions or in normal tissue development.

In stratified epithelia, maintaining homeostasis involves cell death and cellular replacement. Some investigations have focused on desquamation and apoptosis as two mechanisms of cell loss in maintaining homeostasis during regeneration or during the development of stratified epithelia (Shimizu and Yamanaka 1993; Ren and Wilson 1996; Saathof et al. 2004; Lomako et al. 2005). It has been demonstrated that both apoptosis and desquamation are essential and independent processes during epithelial recovery or during development. Postnatal urothelial cell loss was therefore investigated in this study by searching for evidence of apoptosis and desquamation as two key processes of cell elimination.

During mouse and rat development, the urothelium is a rapidly changing tissue that undergoes a series of developmental changes. It has been reported that the urothelial architecture is disrupted for the first time by desquamation of superficial cells at the end of the embrionic period (Firth and Hicks, 1972; Ayres et al. 1985; Cohen et al. 1988). Massive cell desquamation appears again during early postnatal development of mouse urothelium, associated with intense apoptosis, which achieves the peak of its activity on postnatal day 6 (Erman et al. 2001).

It is well known that apoptosis is characterized morphologically by cell shrinkage, disruption of cell–cell contacts, chromatin condensation, membrane blebbing, formation of apoptotic bodies, and, finally, phagocytosis and degradation (Kerr et al. 1972; Wyllie et al.

Correspondence to: Andreja Erman, Institute of Cell Biology, Faculty of Medicine, Lipičeva 2, 1000 Ljubljana, Slovenia. E-mail: andreja.erman@mf.uni-lj.si

Received for publication December 17, 2008; accepted March 27, 2009 [DOI: 10.1369/jhc.2009.953349].

© The Histochemical Society, Inc.

0022-1554/09/$3.30

The Journal of Histochemistry & Cytochemistry

1980; Walker et al. 1988). Biochemically, apoptosis is detected by the presence of endonucleolytical DNA cleavage (Gavrieli et al. 1992; Abend et al. 1998) and cleavage of caspases. Both morphological and biochemical characteristics help in recognizing the presence of apoptotic cells. Caspases are crucial proteases of apoptosis and, among them, activated caspase-3 is well known as a key effector caspase. It cleaves many structural and regulatory proteins and is directly responsible for many of the morphological features of apoptotic cell death (Porter and Jänicke 1999; Steinhusen et al. 2001). Immunohistochemistry and Western blot assay of active caspase-3 were thus performed in the present study, and the morphological features of cells were studied by light and electron microscopy. In addition, the terminal deoxynucleotidyl transferase (TdT)-mediated dUTP nick end labeling (TUNEL) technique was used for the detection of the DNA fragmentation typical of apoptotic cells. The first step in epithelial cell loss is the interruption of cell–cell contacts. Remodeling of junctional contacts and changes of the localization of tight-junction protein occludin were therefore expected and studied. An annexin V/propidium iodide (AnnV/PI) assay was performed to indicate membrane phosphatidylserine exposure in cells released into the lumen of the urinary bladder.

We have developed a special immunohistochemical procedure for observing the urothelial surface on flat tissue pieces with a "bird's-eye view." Using this method, we were able to examine a large area of the luminal urothelial surface involved in cell loss, which is not possible on conventional tissue cross-sections for light microscopy.

The aim of this study was to characterize cell loss in rat postnatal urothelium, focusing on the presence of morphological and biochemical criteria of apoptosis in urothelial cells of the tissue and also in released urothelial cells in the lumen.

Materials and Methods

Animals

Male and female HsdRccHan Wistar rats were used for this study in accordance with European guidelines and Slovenian legislation. Rats were housed at room temperature (22–24C) with 45–65% humidity and a 12-hr light/12-hr dark cycle. Urinary bladders were taken from rats at birth (day 0) to 14 days old (20–32 g), which were euthanized by CO_2 inhalation.

For each method, we sacrificed at least two animals per every postnatal age, with the exception of Western blot analysis and AnnV/PI assay.

Semithin Sections and Transmission Electron Microscopy

Urinary bladders were cut into small pieces and fixed for 3 hr at 4C in a mixture of 4% paraformaldehyde and 2% glutaraldehide in 0.2 M cacodylate buffer (pH 7.3). Overnight rinsing in 0.33 M saccharose in 0.2 M cacodylate buffer was followed by postfixation with 1% osmium tetroxide for 1 hr. After dehydration in ethanol series, tissue samples were embedded in Epon (Serva Electrophoresis; Heidelberg, Germany). Semithin sections of 1-μm thickness were prepared and stained with 1% toluidine blue for examination with a light microscope (Nikon Eclipse TE; Amstelveen, The Netherlands). Ultrathin sections were contrasted with uranyl acetate and lead citrate and examined with a Jeol 100 CX electron microscope.

Scanning Electron Microscopy

Fully filled and distended urinary bladders were excised from animals, cut longitudinally into halves and fixed for 3–4 hr at 4C in a mixture of 2% paraformaldehyde and 2% glutaraldehyde in 0.1 M cacodylate buffer (pH 7.4). The tissue samples were rinsed in 0.1 M cacodylate buffer and postfixed in 1% osmium tetroxide in the same buffer for 1 hr at 4C. Specimens were critical-point dried, sputter-coated with gold, and examined at 15 kV with a Jeol JSM 84 A scanning electron microscope.

Immunostaining on Tissue Sections and on Tissue Pieces

For immunostaining on tissue pieces, fully filled and distended urinary bladders were tightly tied at the base, excised, and fixed for 15 min with 2% paraformaldehyde in PBS buffer, in which they were cut into flat tissue pieces, oriented with the luminal surface of the bladder up. For immunostaining on frozen sections, urinary bladders were frozen and cut into 7-μm-thick frozen sections.

For immunodetection of tight-junction protein occludin and cytokeratin 20 (CK20) as a marker of superficial urothelial cells, fixation with absolute ethanol for 20 min at room temperature was performed, and for immunodetection of β-tubulin, tissue sections were fixed in 4% paraformaldehyde in PBS buffer. After washing in PBS buffer, frozen sections or tissue pieces were permeabilized in 0.4% Triton X-100 for 5 min at room temperature, incubated in 5% fetal calf serum (FCS) and 1% bovine serum albumin (BSA) in PBS buffer for 1 hr at 37C to block nonspecific staining, and incubated overnight at 4C with primary antibodies diluted in 1% BSA as follows: rabbit polyclonal antibodies against occludin (Zymed Laboratories; San Francisco, CA), diluted 1:20; mouse monoclonal antibodies against CK20 (K_s20.8; Dako, Glostrup, Denmark), diluted 1:100; and rabbit polyclonal antibodies against β-tubulin, diluted 1:100 (Sigma; Taufkirchen, Germany). As negative controls, primary antibodies were omitted or replaced with PBS buffer. After washing in PBS buffer (three times for 10 min), samples were incubated with

The Journal of Histochemistry & Cytochemistry

adequate secondary antibodies tetramethyl rhodamine iso-thiocyanate (TRITC)-labeled goat anti-rabbit (Alexa Fluor 555; Invitrogen, Molecular Probes, Leiden, the Netherlands) or FITC-labeled goat anti-rabbit (Alexa Fluor 488; Invitrogen, Molecular Probes) and TRITC-labeled or FITC-labeled rabbit anti-mouse (Sigma) diluted 1:200 in 1% BSA for 1 hr at 37C in the dark. After washing in PBS buffer three times for 10 min, the samples were mounted in the mounting medium Vectashield with 4′,6-diamidino-2-phenylindole (DAPI; Vector Laboratories, Burlingame, CA) and observed with a Nikon Eclipse TE 300 fluorescence microscope.

For immunodetection of active caspase-3 on frozen sections, endogenous peroxidase activity was blocked by incubation in 3% H_2O_2 in methanol for 15 min. After washing in PBS buffer, slides were treated with 5% FCS and 1% BSA in PBS buffer for 1 hr at 37C to block nonspecific staining and incubated overnight at 4C with primary rabbit polyclonal antibodies (Abcam; Cambridge, UK) diluted 1:100 in 1% BSA. As a negative control, primary antibodies were replaced with PBS buffer. After washing in PBS buffer, biotinylated swine anti-rabbit immunoglobulins (Dako), diluted 1:100, were applied for 1 hr at room temperature, followed by incubation with avidin:biotinylated enzyme complex/horseradish peroxidase (HRP; Dako) for 30 min at room temperature. After the standard DAB (Sigma) procedure, sections were stained in Mayer's hematoxylin, dehydrated, mounted in Depex, and examined with a Nikon Eclipse TE 300 light microscope.

For immunofluorescent detection of active caspase-3 on tissue pieces, permeabilization in 0.4% Triton X-100 for 5 min at room temperature was performed, followed by incubation in 5% FCS and 1% BSA in PBS buffer for 1 hr at 37C to block nonspecific staining. Tissue pieces were incubated overnight at 4C in rabbit polyclonal antibodies against active caspase-3 (R and D Systems; Wiesbaden, Germany) diluted 1:500 in 1% BSA. As a negative control, primary antibodies were replaced with PBS buffer. After washing in PBS buffer, samples were incubated with secondary TRITC-labeled goat anti-rabbit antibodies (Alexa Fluor 555; Invitrogen, Molecular Probes), diluted 1:200 in 1% BSA, for 1 hr at 37C in the dark. After washing in PBS buffer, the samples were mounted in the mounting medium Vectashield with DAPI (Vector Laboratories) and observed with a Nikon Eclipse TE 300 fluorescence microscope.

For actin filaments staining on tissue pieces, urinary bladders were fixed for 30 min with 4% paraformaldehyde immediately after excision and cut into flat tissue pieces in the fixative solution. After washing in PBS, tissue pieces were incubated with FITC-labeled phalloidin diluted 1:8 with PBS buffer (Sigma) for 1 hr at 37C in the dark. After washing in PBS (three times for 10 min), tissue pieces were mounted in the mounting medium Vectashield with DAPI (Vector Laboratories) and observed with a Nikon Eclipse TE 300 fluorescence microscope.

In Vivo Detection of Apoptosis With a FLIVO Kit

Detection of active caspases in urothelial cells by an in vivo technique was performed in accordance with the manufacturer's instructions (FAM-FLIVO in vivo apoptosis reagent; Immunochemistry Technologies, LLC, Bloomington, MN). The reagent, cell permeant poly caspase binding inhibitor probe (FAM-VAD-FMK), enters the cell and forms an irreversible covalent bond only with active caspases, whereas the unbound reagent is quickly cleared from the non-apoptotic cells. Because of the reagent segment FAM, which is a fluorescent label, apoptotic cells or active caspase-positive cells fluoresce green.

The reagent was diluted in dimethyl sulfoxide and sterile injection buffer, and 40 μl of prepared reagent solution was injected intravenously through the femoral vein of a young rat. After 30 min, when the reagent had circulated throughout the body, the urinary bladder was excised. Some fully filled and stretched urinary bladders were fixed in 2% paraformaldehyde and cut into flat pieces, and the others were immediately frozen and cut into 7-μm-thick frozen sections. Flat tissue pieces and frozen sections were mounted in the mounting medium Vectashield with DAPI (Vector Laboratories) and observed with a Nikon Eclipse TE 300 fluorescence microscope. The small intestine of young rats was taken for positive control.

Western Blot Analysis

Urinary bladders were cut into pieces, which were incubated in a solution of Dispase I (neutral protease, grade I; Roche, Mannheim, Germany), with a working concentration of 1.2 U/ml, for 90 min at 37C. After that time, intact urothelial sheets were easily picked up from underlying tissue and homogenized in ice-cold buffer (0.8 M Tris-HCl, 7.5% SDS, 1 mM PMSF). The homogenate was centrifuged, and the protein concentration in the supernatant was determined using a BCA protein assay kit (Pierce; Rockford, IL). Sample proteins (30 μg/lane) were size fractionated on 7.5%, 12%, or 15% SDS-polyacrylamide gels and then transferred to Hybond enhanced chemoluminescence (ECL) nitrocellulose membranes (Amersham Biosciences, Little Chalfont, UK) by electroblotting. After blocking overnight at 4C (in 5% skim milk in PBS-Tween), membranes were incubated for 2 hr at room temperature with primary rabbit polyclonal antibodies against active caspase-3 (R and D Systems) diluted 1:2000. After washing in PBS-Tween (four times for 5 min), membranes were incubated for 1 hr with HRP-conjugated goat anti-rabbit antibodies

The Journal of Histochemistry & Cytochemistry

(Sigma) diluted 1:1000. Membranes were finally probed with ECL reagent (Amersham Biosciences) and exposed to X-ray films. Rabbit anti-actin antibodies diluted 1:1000 (Sigma) were used to confirm an equal loading of protein in each lane. As negative controls, the primary antibodies were omitted.

For each analysis, five animals of the last embryonic age (embryonic day 22), three animals of every postnatal age between day 7 and day 10, and two adult animals were sacrificed.

Analysis of Cell Death by AnnV/PI Assay

Urinary bladders were exposed, and the urine, together with floating cells, was needle aspirated. The urine from 20 young rats of the same age was collected. AnnV/PI staining was performed in accordance with the manufacturer's instructions (annexin-V-FLUOS staining kit; Roche). Cells in the urine were washed in PBS, centrifuged at 200 × g for 5 min, resuspended in labeling solution [2 μl AnnV-FITC, 2 μl PI, and 100 μl incubation buffer (HEPES)] and incubated for 15 min in the dark at room temperature. Stained cytological samples, mounted in the mounting medium Vectashield (Vector Laboratories) were examined with a fluorescence microscope.

AnnV-fluos highly and specifically binds to phosphatidylserine, which is exposed on the outer leaflet of the plasma membrane of apoptotic and necrotic cells, whereas propidium iodide stains DNA of leaky necrotic cells only. This assay was used to define urothelial cells in the lumen as apoptotic or necrotic. We defined four types of cells according to the fluorescence emission of collected cells: viable intact cells (AnnV−/PI−), apoptotic cells (AnnV+/PI−), late apoptotic/early necrotic cells (AnnV+/PI+), and necrotic/dead cells (Ann−/PI+).

TUNEL Assay

Pieces of urinary bladders were fixed in 4% paraformaldehyde in PBS at 4C overnight, dehydrated, and embedded in paraffin. Sections 5 μm thick were cut and mounted on aminopropyltriethoxysilane-coated glass slides. After deparaffinization and dehydration, the sections were treated with 20 μg/ml proteinase K (Boehringer Mannheim, Germany) in PBS for 15 min at room temperature. After rinsing with distilled water, the sections were briefly incubated in the solution of 0.1% Triton X-100 in 3.4 mM Na-citrate and rinsed again in PBS. Endogenous peroxidase activity was blocked with 0.5% H_2O_2 in PBS for 20 min at room temperature. The sections were then rinsed in PBS three times, preincubated in a solution of 200 mM N a-cacodylate, 0.25 mg/ml BSA, and 0.3 mM $CoCl_2$ in 25 mM Tris-HCl for 10 min at room temperature, and then treated with TdT (0.1 U/μl; Boehringer Mannheim) and digoxigenin-11-dUTP (dilution 1:25; Boehringer Mannheim) in 25 mM Tris-HCl with 0.1 mM $CoCl_2$ for 1 hr at 37C. The reaction was terminated by a solution of 300 mM NaCl and 30 mM Na-citrate for 30 min at 37C. The sections were rinsed with PBS three times and incubated in the anti-digoxigenin peroxidase-conjugated antibodies (dilution 1:300; Boehringer Mannheim) and 1% blocking reagent (Boehringer Mannheim) for 30 min at room temperature. After washing in PBS, the reaction was visualized by a 0.1% DAB solution (Sigma) and stained with Mayer's hematoxylin. As negative controls, TdT was omitted, and as positive controls, sections were pretreated with DNase.

Results

Light and electron microscopy revealed that apoptosis took place in the urothelium throughout the early postnatal period, from the day of birth until day 14 (Figures 1A and 1B), whereas desquamation appeared only between postnatal days 7 and 10 (Figures 2A and 2B). Only during these few days did urothelial cells undergo apoptosis and desquamation simultaneously (Figures 3A and 3B).

In the urothelium, between postnatal days 7 and 10, numerous apoptotic bodies were detected by light and electron microscopy, phagocytosed in the cytoplasm of mostly intermediate urothelial cells (Figure 4A) or extruded from the urothelium and exposed on the urothelial luminal surface (Figure 4B). Many cells in tissue with TUNEL-stained nuclei showed DNA fragmentation (Figure 5). Activated caspases were detected by the FLIVO kit for detecting active caspases in situ (Figure 6). Active caspase-3 was also found in the cytoplasm of urothelial cells by immunodetection of this enzyme (Figures 7A and 7B), and its presence was confirmed by Western blot analysis (Figure 8).

Disassembled cell–cell contacts between urothelial superficial cells were detected on the urothelial surface only between postnatal days 7 and 10 (Figure 9A). Immunodetection of tight-junction protein occludin showed strong staining of two fluorescent sharp lines at cell–cell boundaries, indicating that cell–cell junctions were disconnected between superficial cells that had started to desquamate (Figure 9B). As a consequence of the cleavage of cell–cell contacts, enlarged intercellular spaces appeared between superficial cells (Figures 9A and 9C) or between superficial and underlying cells (Figures 9C and 10A). Superficially located intermediate cells were exposed on the urothelial surface after the elimination of desquamating "old" superficial cells (Figures 10A and 10B). Urothelial cells desquamated individually and in groups of superficial cells or in superficial and underlying cells together. On several luminal surface areas, therefore, the urothelium was peeled off due to massive desquamation (Figures 11A–11D).

The Journal of Histochemistry & Cytochemistry

Figures 1–4

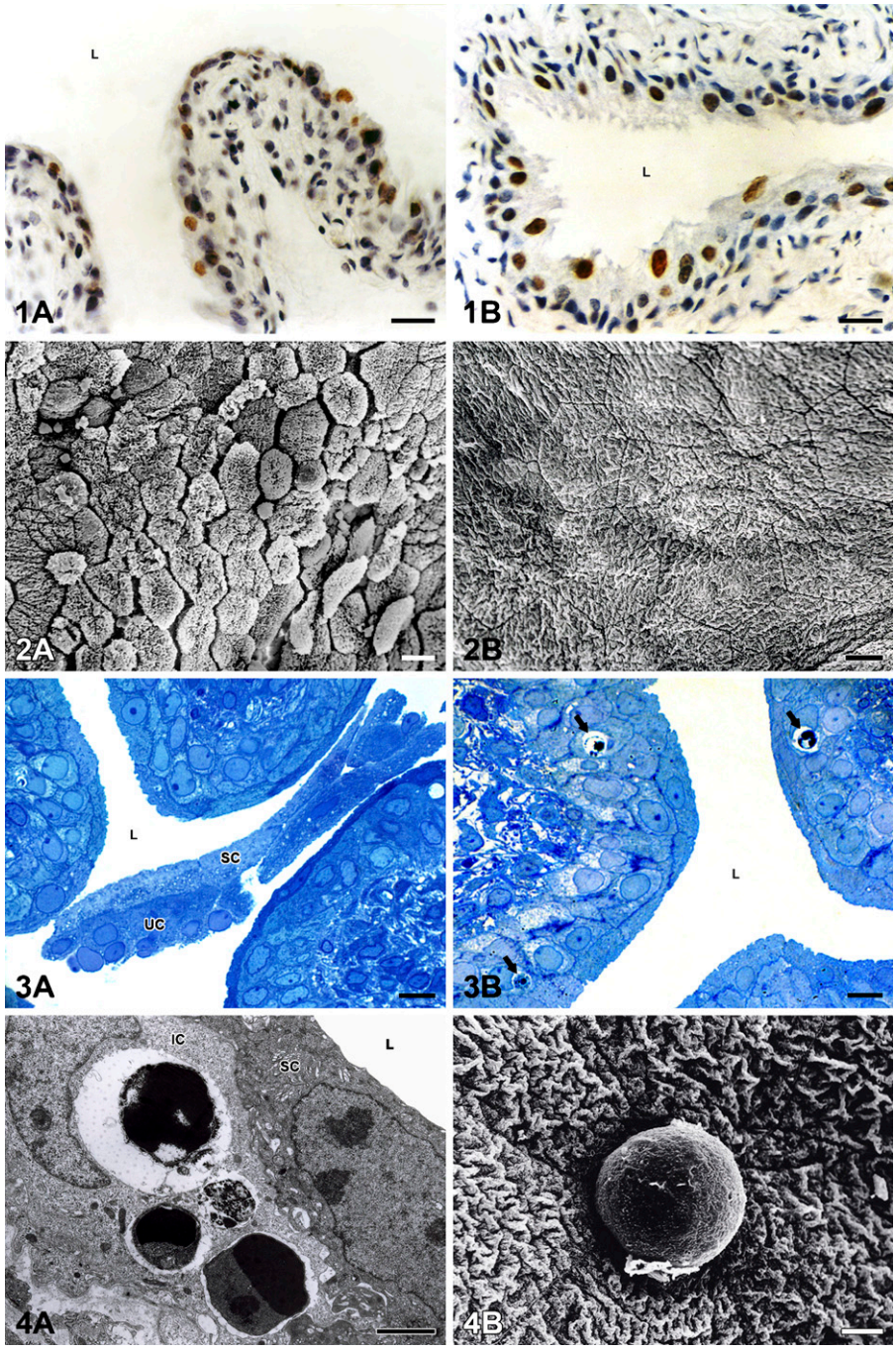

Figure 1 Numerous terminal deoxynucleotidyl transferase–mediated dUTP nick end labeling (TUNEL)-positive urothelial cells with brown-colored nuclei are present in the urothelium before and after the period of desquamation. (**A**) Postnatal day 1. (**B**) Postnatal day 14. Nuclei are stained with hematoxylin. L, lumen of the urinary bladder. Bar = 40 μm.

Figure 2 Massive desquamation takes place in the urothelium on postnatal day 10 (**A**). After that day, the urothelium is non-desquamating tissue with tightly joined cells and luminal surface of normal and specific appearance. (**B**) Postnatal day 14. Bar = 20 μm.

Figure 3 Semithin sections of the urothelium on postnatal day 7. Numerous desquamated superficial (SC) and underlying (UC) urothelial cells in the lumen (L) of the urinary bladder (**A**). Phagocytosed apoptotic bodies (arrows) in the cytoplasm of intermediate urothelial cells (**B**). Bar = 10 μm.

Figure 4 Detection of apoptotic bodies by transmission electron microscopy (TEM) and scanning electron microscopy (SEM). (**A**) Phagocytosed apoptotic bodies in the cytoplasm of intermediate urothelial cell (IC), detected by TEM on postnatal day 7. SC, superficial cell; L, lumen of the urinary bladder. (**B**) Apoptotic body on the luminal surface of the urothelium, detected by SEM on postnatal day 7. Bars: **A** = 5 μm; **B** = 10 μm.

Released urothelial cells detected in the lumen of the urinary bladder between postnatal days 7 and 10 revealed various morphological and biochemical properties. The majority of them showed typical biochemical criteria of apoptosis, such as the presence of activated caspases, detected by a FLIVO kit (Figure 12), and the activation of caspase-3, proved by the immunostaining of this enzyme (Figures 13A and 13B). DNA fragmentation was also revealed in many desquamated, TUNEL-positive cells in the lumen (Figure 14).

Examination under light and electron microscopy proved that desquamating and desquamated cells in the lumen of the bladder retained their size and shape and showed no morphological hallmarks of apoptosis, such as characteristic apoptotic nuclear condensation, cell shrinkage, and membrane blebbing (Figures 3A, 11C,

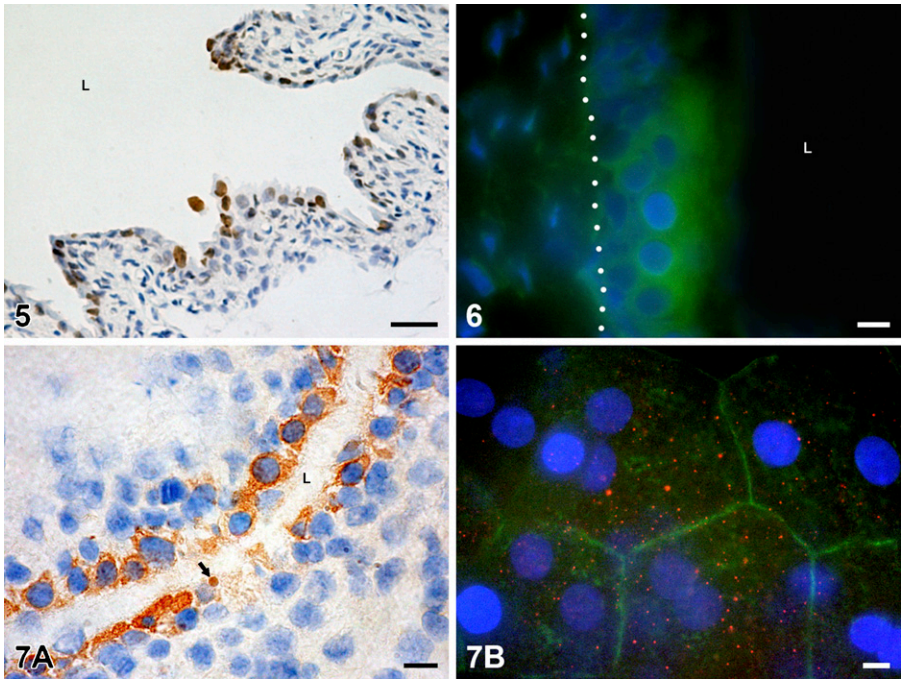

Figures 5–7

Figure 5 Many TUNEL-positive cells with brown-colored nuclei are detected in the urothelium on postnatal day 7. Nuclei are stained with hematoxylin. L, lumen of the urinary bladder. Bar = 40 μm.

Figure 6 Detection of active caspases in situ in the urothelium by FLIVO kit. An area of intact three-layered urothelium shows caspase activity (green). Tissue section on postnatal day 10. Basal lamina is marked with a dotted line. Nuclei are stained with 4′,6-diamidino-2-phenylindole (DAPI). L, lumen of the urinary bladder. Bar = 10 μm.

Figure 7 Immunodetection of active caspase-3 in the urothelium. (**A**) Brown color shows positive reaction in the cytoplasm of the majority of urothelial cells and in one apoptotic body (arrow) in the tissue section on postnatal day 7. Nuclei are stained with hematoxylin. L, lumen of the urinary bladder. (**B**) Positive reaction is manifested as red dots (red fluorescence) in the cytoplasm of superficial cells. Actin filaments (green fluorescence) are arranged as a cortical belt close to the cell borders. Bird's-eye view of the luminal urothelial surface on the tissue piece, postnatal day 10. Nuclei are stained with DAPI. Bar = 10 μm.

13B, 15, and 16A). The results of the AnnV/PI assay of released urothelial cells collected in the lumen revealed large, polygonal, binucleated cells in the lumen, which were AnnV+/PI+, indicating that these cells had undergone late apoptosis or early necrosis (Figure 16A). Small, rounded, AnnV+/PI− apoptotic bodies were also found among them, in the lumen of the urinary bladder (Figure 16B).

Discussion

In mouse urothelial development, the first comprehensive desquamation of urothelial cells takes place at the end of the embryonic period, and a second one appears in the early postnatal period (Ayres et al. 1985; Erman et al. 2001). During the first five postnatal days, which represent the period between the two main destructions in development, the structure of the urothelium is of a short-term and "transitional" character (Erman et al. 2006). Namely, between postnatal days 6 and 9, intense repeated desquamation eliminates these transitional neonatal urothelial cells. The ensuing restoration ultimately leads to the terminally differentiated urothelium seen in the adult animal.

In this study, we embarked on the analysis of urothelial cell elimination in the rat. Our goal was to clarify the nature of cell loss in postnatal rat urothelium by determining the morphological and biochemical characteristics of cells in the urothelium and of released cells. During the early postnatal period (from the day of birth to postnatal day 14), rat urothelial cells were eliminated from the tissue by apoptosis, autophagic cell death, and desquamation. Apoptosis was detected throughout the first 14 days, whereas only occasional

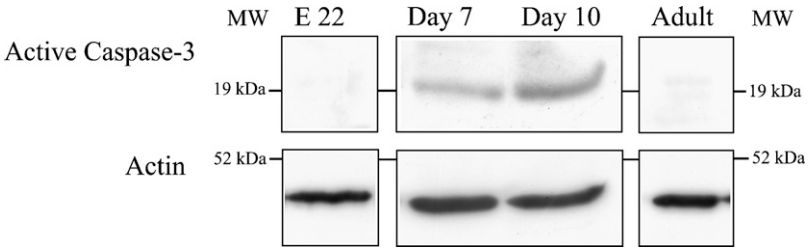

Figure 8 Western blot analysis of active caspase-3 in urothelial cells on embryonic day 22 and on postnatal days 7 and 10 and in adult animals. Antibody against active caspase-3 recognizes the fragment of 17–20 kDa of a larger subunit after proteolytical cleavage of the inactive enzyme. Active form of caspase-3 is present at the position corresponding to 19 kDa on both postnatal days, but is absent on embryonic day 22 and in adult animals. Immunoblot experiments were performed twice with similar results. MW, molecular weight standards.

The Journal of Histochemistry & Cytochemistry

Figures 9–11

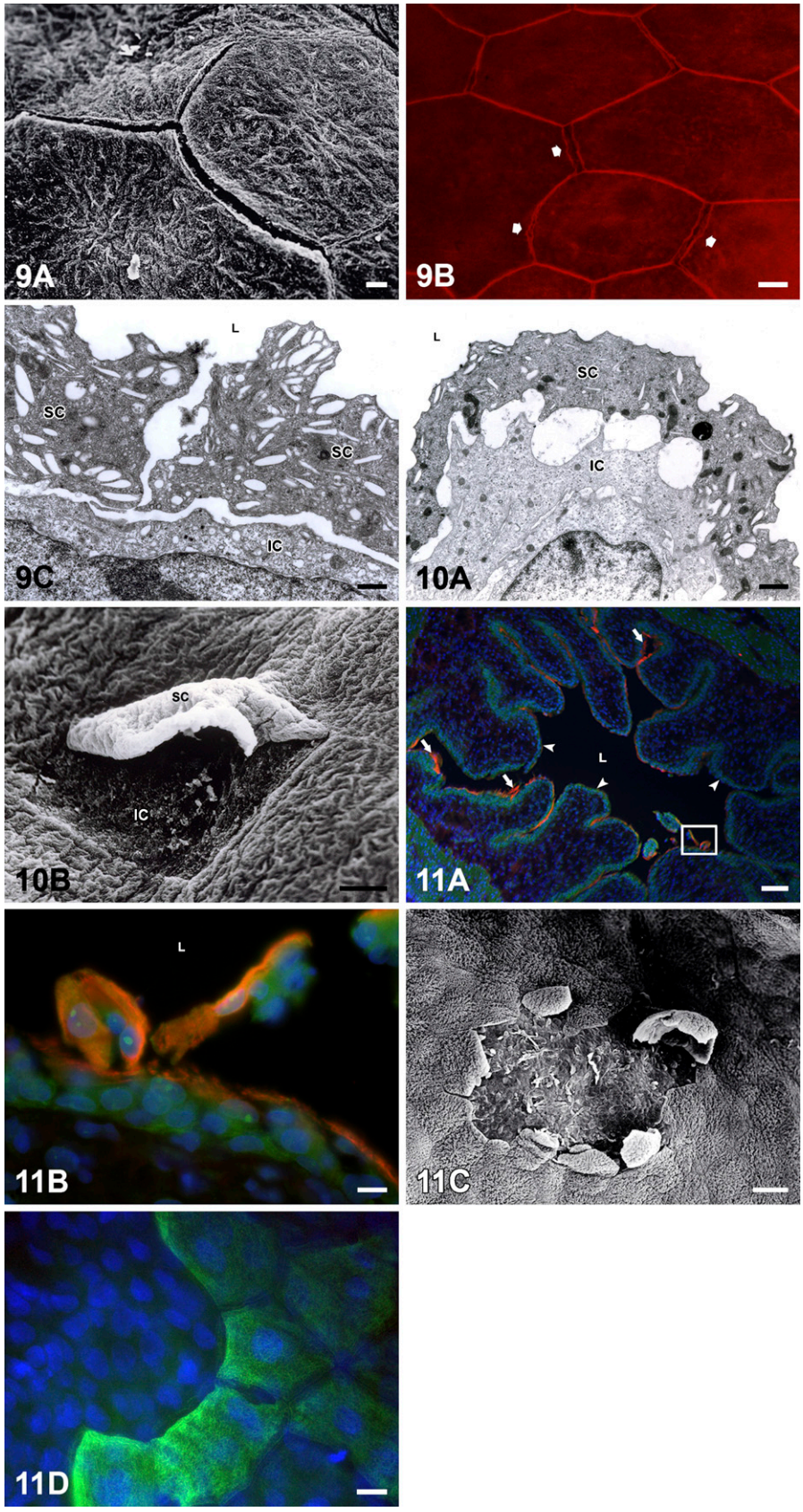

Figure 9 Disassembled cell–cell junctions during urothelial cell desquamation. (**A**) Exposed gaps between superficial urothelial cells due to cleaved cell–cell junctions, detected by SEM on postnatal day 8. (**B**) Immunostaining of tight-junction protein occludin (red fluorescence) reveals doubled cell–cell boundaries and exposed gaps (arrows) between superficial cells, indicating the beginning of cell desquamation. Bird's-eye view of the luminal urothelial surface on the tissue piece, postnatal day 8. (**C**) Enlarged intercellular spaces between two neighboring superficial cells (SC) and between superficial and intermediate cell (IC) detected by TEM on postnatal day 8. L, lumen of the urinary bladder. Bars: **A,B** = 10 μm; **C** = 2 μm.

Figure 10 TEM image shows superficial urothelial cell (SC) during the detachment and intermediate cell (IC), which will be superficially located and will replace "old" desquamating superficial cell immediately after its final detachment (**A**). L, lumen of the urinary bladder. (**B**) SEM image of desquamating superficial cell (SC), which is still partly attached to the neighboring cells. Under this cell, an intermediate cell (IC) is already partly exposed on the urothelial surface. Bars: **A** = 2 μm; **B** =20 μm.

Figure 11 Postnatal urothelial cell desquamation. (**A**) Cytokeratin 20 (CK20)-positive superficial cells (red, immunolabeled by antibodies against CK20) and CK20-negative intermediate cells (green, immunolabeled by antibodies against β-tubulin) desquamated in the lumen of the urinary bladder. In certain areas of the urothelium, superficial cells are still attached to the urothelium (arrows), whereas other areas of the urothelium are already peeled off, owing to cell desquamation (arrowheads). Detail in the frame is enlarged in **B**. Nuclei are stained with DAPI. Tissue section on postnatal day 10. L, lumen of the urinary bladder. (**B**) Enlarged, mirror-inverted detail of **A** shows desquamation of superficial cells (red fluorescence) and occasional underlying cells (green fluorescence) in the lumen (L) of the urinary bladder. Nuclei are stained with DAPI. (**C**) SEM image shows desquamated area of the urothelium. At the edge of this area, some desquamating cells are partly still attached to the urothelium. Postnatal day 8. (**D**) Immunostaining of CK20 (green fluorescence) shows intact luminal urothelial surface on the right and desquamated area with no superficial cells on the left side of the figure. Bird's-eye view of the luminal urothelial surface of the tissue piece. Postnatal day 10. Nuclei are stained with DAPI. Bars: **A** = 100 μm; **B–D** = 10 μm.

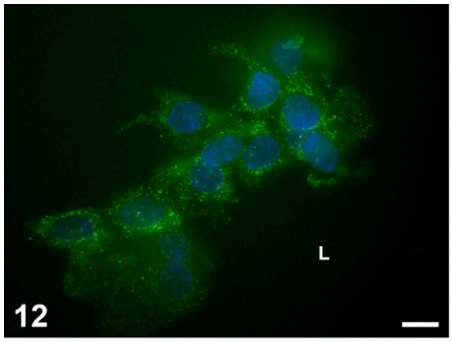

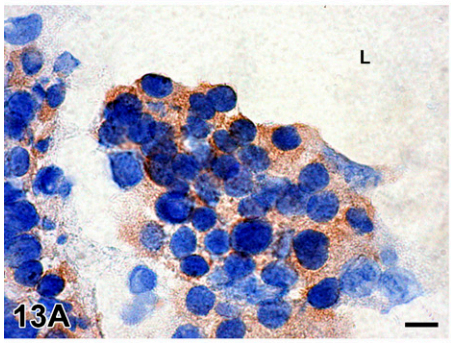

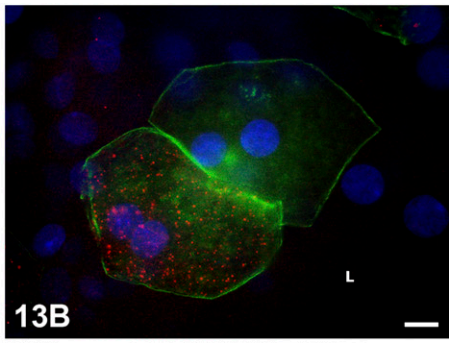

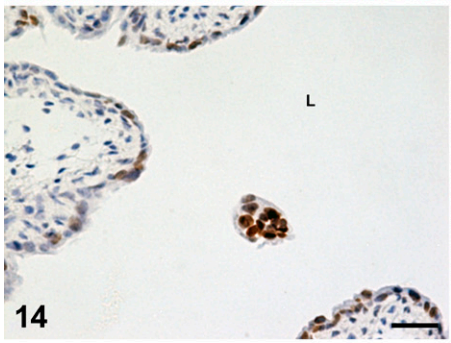

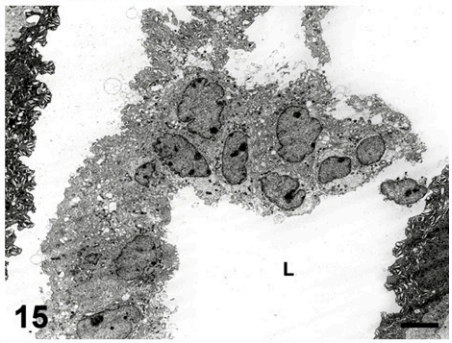

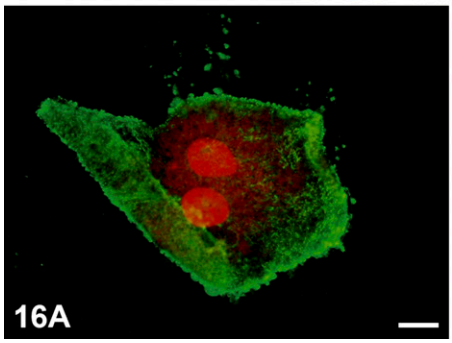

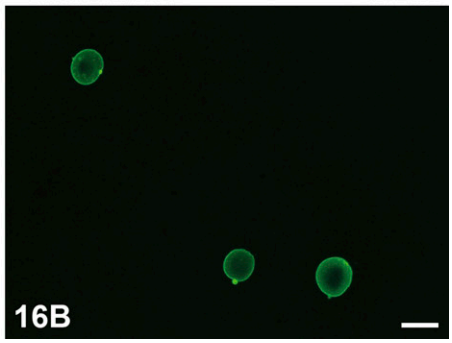

Figures 12–16

Figure 12 Detection of active caspases in situ in desquamated cells in the lumen of the urinary bladder by FLIVO kit. Urothelial cells released from the urothelium fluoresce green, owing to fluorescent reagent, and bond to activated caspases. Tissue piece on postnatal day 10. Nuclei are stained with DAPI. L, lumen of the urinary bladder. Bar = 10 μm.

Figure 13 Detection of active caspase-3 in desquamated cells. (**A**) In a group of desquamated cells, the majority show a positive cytoplasmic reaction (brown color). Tissue section on postnatal day 7. Nuclei are stained with hematoxylin. (**B**) Two superficial polygonal and binucleated cells detected in the lumen after desquamation from the tissue piece on postnatal day 7. One of them shows positive dotty reaction against active caspase-3 (red fluorescence). Actin filaments fluoresce green. Nuclei are stained with DAPI. L, lumen of the urinary bladder. Bar = 10 μm.

Figure 14 A group of desquamated cells with TUNEL-positive nuclei in the lumen (L) of the urinary bladder on postnatal day 7. Nuclei are stained with hematoxylin. Bar = 40 μm.

Figure 15 Desquamated cells in the lumen of the urinary bladder show no morphological features of apoptosis. Ultrathin section on postnatal day 7. L, lumen of the urinary bladder. Bar = 10 μm.

Figure 16 Fluorescent annexin V/propidium iodide (AnnV/PI) assay with annexin V (green labeling) and PI (red labeling) of released urothelial cells. (**A**) Desquamated superficial binucleated AnnV+/PI+ cell, which retains its typical polygonal shape and size. Postnatal day 7. (**B**) The image shows three small, rounded apoptotic bodies, which are Ann+/PI−. Postnatal day 7. Bars: **A** = 30 μm; **B** = 10 μm.

superficial cells underwent autophagic cell death in this period. This form of programmed cell death remains to be elucidated in our further studies. Massive desquamation, which was the focus of the present study, was detected with light and electron microscopy between postnatal days 7 and 10, when superficial cells desquamate individually or in groups with intermediate cells, into the lumen of the urinary bladder. Immunofluorescent detection of occludin as a protein of tight junctions revealed a positive reaction as two fluorescent sharp lines at superficial cell borders and around exposed gaps between these cells. This situation was detected on the surface of the urothelium only between postnatal days 7 and 10, and it represented clear evidence of the begining of desquamation of urothelial cells.

During the same postnatal period, intense apoptotic activity of cells in the intermediate layer was detected by light and electron microscopy. Numerous apoptotic

The Journal of Histochemistry & Cytochemistry

bodies were found in deeper urothelial layers, mostly phagocytosed by intermediate cells or extruded into the lumen of the bladder. Not even one apoptotic cell was visible in the urothelium, proving that apoptosis is a fast process and the clearance time is very short. Superficial cells in the urothelium or released into the lumen showed no typical morphological hallmarks of apoptosis. Biochemical identification of apoptosis was performed by immunohistochemical detection of active caspases and Western blot assay of active caspase-3. Our results of immunodetection and Western blot assay prove that caspase-3 was active in the urothelium and in the majority of desquamated cells, but not in all. We assume that this is because cells with activated caspase-3 started to lose cell–cell contacts and release from the urothelium, whereas neighboring cells with inactivated caspases were passively pulled into the lumen. It is well known that the disassembling of cell–cell contacts is a consequence of metalloprotease or caspase activity, which splits cell junction proteins, and several of them have already been shown to be targets of caspase-3 (Steinhusen et al. 2001; Weiske et al. 2001; Bojarski et al. 2004; Gregorc et al. 2007).

The major advantage of apoptosis detection in situ with a FLIVO kit was that we did not induce postmortem apoptosis artificially by killing the animal or by removing tissue from the animal. The results of this technique additionally confirm the results of active caspase-3 immunostaining, showing caspase activity in certain areas of the urothelium and also in desquamated cells in the lumen.

The results of TUNEL staining were also in agreement with the detection of active caspases, because we detected TUNEL-positive cells with DNA fragmentation in the urothelium and in desquamated cells in the lumen of the bladder. Although we proved caspase activity and DNA fragmentation in desquamated cells, these cells did not exhibit typical morphological criteria of apoptosis, such as cell shrinkage, apoptotic chromatin condensation, or membrane blebbing.

We also performed an AnnV/PI assay to detect membrane phosphatidylserine exposure in cells collected in the lumen of the bladder after the release from the urothelium (Vermes et al. 1995; Baskiæ et al. 2006). This assay identified small, rounded, AnnV+/PI− apoptotic bodies and many large, polygonal, AnnV+/PI+ cells in the bladder lumen. AnnV+/PI− apoptotic bodies are remnants of cells that underwent apoptosis in the urothelium and were extruded from the tissue as apoptotic bodies in the bladder lumen. Apoptotic bodies were also detected in the extrusion phase under scanning electron microscopy. The second type of cells in the lumen were AnnV+/PI+ cells. These cells were late apoptotic or early necrotic. They preserved the same shape and size that they had in the intact urothelium. Unchanged shape and size and the absence of typical morphological characteristics of apoptosis prove that these cells did not die in an apoptotic manner but were eliminated from the urothelium by desquamation. On the other hand, biochemical characteristics such as caspase cleavage and DNA cleavage were confirmed in the majority of desquamated cells. Cell desquamation could thus be an apoptotic event that does not reflect the late morphological features of apoptotic death, owing to the fast release from the urothelium. However, a definitive conclusion concerning apoptosis as an inducer of urothelial cell desquamation is beyond the aim of this study.

Urothelial cells die in an apoptotic manner throughout embryonic and postnatal development, contributing to maintained tissue homeostasis. On the other hand, intense apoptotic activity and massive desquamation are present simultaneously only during a few postnatal days in rat urothelium. It seems that intense apoptosis and cell desquamation are both essential for efficient urothelial remodeling and fast elimination of transitional neonatal urothelium, as in the mouse. Urothelial cells of deeper cell layers undergo apoptosis, whereas superficial cells abundantly desquamate into the lumen. Desquamation obviously represents a faster, more economical, and more efficient mechanism of superficial cell loss than does apoptosis.

Acknowledgments

This study was supported by Slovenian Research Agency (ARRS) grant P3-0108.

The authors thank Martina Perše, DVM, animal welfare officer at the Medical Experimental Centre of the Faculty of Medicine in Ljubljana for professional advice and technical help in performing the experiments with the FLIVO kit. We also thank Martin Cregeen for correcting the English text.

Literature Cited

Abend M, Schmelz HU, Kraft K, Rhein AP, van Beuningen D, Sparwasser C (1998) Intercomparison of apoptosis morphology with active DNA cleavage on single cells in vitro and on testis tumours. J Pathol 185:419–426

Aronson M, Medalia O, Amichay D, Nativ O (1988) Endotoxin-induced shedding of viable uroepithelial cells is an antimicrobial defence mechanism. Infect Immun 56:1615–1617

Ayres PH, Shinohara Y, Frith CH (1985) Morphological observations on the epithelium of the developing urinary bladder of the mouse and rat. J Urol 133:506–512

Baskić D, Popović S, Ristić P, Arsenijević NN (2006) Analysis of cycloheximide-induced apoptosis in human leukocytes: fluorescence microscopy using annexin V/propidium iodide versus acridin orange/ethidium bromide. Cell Biol Int 30:924–932

Bojarski C, Weiske J, Schöneberg T, Schröder W, Mankertz J, Schulzke JD, Florian P, et al. (2004) The specific fate of tight junction proteins in apoptotic epithelial cells. J Cell Sci 117:2097–2107

Cohen SM, Cano M, Sakata T, Johansson SL (1988) Ultrastructural characteristics of the fetal and neonatal rat urinary bladder. Scanning Microsc 2:2091–2104

Dalal E, Medalia O, Harasi O, Aronson M (1994) Moderate stress protects female mice against bacterial infection of the bladder by eliciting uroepithelial shedding. Infect Immun 62:5505–5510

Erman A, Štiblar-Martinčič D, Romih R, Veranič P, Jezernik K (2001) Postnatal restoration of the mouse urinary bladder urothelium. Histochem Cell Biol 115:309–316

Erman A, Veranič P, Pšeničnik M, Jezernik K (2006) Superficial cell differentiation during embryonic and postnatal development of mouse urothelium. Tissue Cell 38:293–301

Firth JA, Hicks RM (1972) Membrane specialization and syncronized cell death in developing rat transitional epithelium. J Anat 113:95–107

Gavrieli Y, Sherman Y, Ben-Sasson SA (1992) Identification of programmed cell death in situ via specific labeling of nuclear DNA fragmentation. J Cell Biol 119:493–501

Gregorc U, Ivanova S, Thomas M, Guccione E, Glaunsinger B, Javier R, Turk V, et al. (2007) Cleavage of MAG-1, a tight junction PDZ protein, by caspases is an important step for cell-cell detachment in apoptosis. Apoptosis 12:343–354

Kerr JFR, Wyllie AH, Currie AR (1972) Apoptosis: a basic biological phenomenon with wide-ranging implication in tissue kinetics. Br J Cancer 26:239–257

Lomako J, Lomako WM, Decker SJ, Carothers Carraway CA, Carraway KL (2005) Non-apoptotic desquamation of cells from corneal epithelium: putative role for Muc4/Sialomucin complex in cell release and survival. J Cell Physiol 202:115–124

Porter AG, Jänicke RU (1999) Emerging roles of caspase-3 in apoptosis. Cell Death Differ 6:99–104

Ren H, Wilson G (1996) Apoptosis in the corneal epihelium. Invest Ophthalmol Vis Sci 37:1017–1025

Saathof M, Blum B, Quast T, Kirfel G, Herzog V (2004) Simultaneous cell death and desquamation of the embryonic diffusion barrier during epidermal development. Exp Cell Res 299: 415–426

Shimizu A, Yamanaka N (1993) Apoptosis and cell desquamation in repair process of ischemic tubular necrosis. Virchows Arch B Cell Pathol 64:171–180

Steinhusen U, Weiske J, Badock V, Tauber R, Bommert K, Huber O (2001) Cleavage and shedding of E-cadherin after induction of apoptosis. J Biol Chem 276:4972–4980

Veranič P, Jezernik K (2000) The response of junctional complexes to induced desquamation in mouse urinary bladder urothelium. Biol Cell 92:105–113

Veranič P, Jezernik K (2001) Succession of events in desquamation of superficial cells as a response to stress induced by prolonged constant illumination. Tissue Cell 33:280–285

Vermes I, Haanen C, Steffens-Nakken H, Reutelingsperger C (1995) A novel assay for apoptosis. Flow cytometric detection of phosphatidylserine expression on early apoptotic cells using fluorescein labelled Annexin V. J Immunol Methods 184:39–51

Walker NI, Harmon BV, Gobé GC, Kerr JFR (1988) Patterns of cell death. Methods Achiev Exp Pathol 13:18–54

Weiske J, Schöneberg T, Schröder W, Hatzfeld M, Tauber R, Huber O (2001) The fate of desmosomal proteins in apoptotic cells. J Biol Chem 276:41175–41181

Wyllie AH, Kerr JFR, Currie AR (1980) Cell death: the significance of apoptosis. Int Rev Cytol 68:251–306

The Journal of Histochemistry & Cytochemistry